Electronic Supplementary Material (ESI) for Inorganic Chemistry Frontiers.

Magnifying turn-on luminescence and electrical conductivity by coupling effect among oxidation, metal ions adhesion and pressure within Mn^{II}-MOFs

Ting-chang Shi,[⊥a] Zhi-hui Li,[⊥b] Zhiyue Dong, Ming-Hua Zeng*[a,b] and Hai-Bing Xu*[a,c]

[a] Hubei Collaborative Innovation Center for Advanced Organic Chemical Materials, Ministry-of-Education Key Laboratory for the Synthesis and Application of Organic Functional Molecules & College of Chemistry & Chemical Engineering, Hubei University, Wuhan, 430062, P.R. China.

[b] Department of Chemistry and Pharmaceutical Sciences, Guangxi Normal University, Key laboratory for the Chemistry and Molecular Engineering of Medicinal Resources, Guilin, 541001, P.R. China.

⊥ These authors contributed equally to this work.

KEYWORDS "Multi-responsive fluorescent sensor", "Post-synthetic modification", "Turn-on sensing behavior", "Coupling effect", "Luminescent MOFs"

EXPERIMENTAL SECTION

Reagents

The reagents employed in this experiment, including 4-carboxyphenylboronic acid, 4,7-dibromo-2,1,3-benzothiadiazole, tetrakis(triphenylphosphine)palladium ($Pd[P(C_6H_5)_3]_4$), acetonitrile, cesium fluoride (CsF), manganese chloride ($MnCl_2$), as well as other high-chloride and nitrate salts, were procured from Adamas (Switzerland). Methanol, hydrochloric acid (HCl), dimethoxyethane (DME), dichloromethane (CH_2Cl_2), and acetone were purchased from China National Pharmaceutical Group Chemical Reagent Co., Ltd (China). Acetic ether and petroleum ether, used as chromatographic column solvents, were obtained from XINSHENSHI Reagent Co., Ltd (China).

Materials Preparation

Hydrothermal synthesis of **Mn1**. A dimethylformamide (DMF) solution (9 mL) containing $MnCl_2 \cdot 4H_2O$ (99 mg, 0.5 mmol), 4,4'-(1,2,5-benzothiadiazole-4,7-diyl)bis-Benzoic acid (btdb) (47 mg, 0.125 mmol) in a 15 mL teflon-lined steel bomb was heated at 140 °C for 48 h. The autoclave was cooled at a rate of 10 °C h^{-1}, light yellow needle crystals (**Mn1**) were collected, Yield: 34% (based on Mn) (Figure S1). The phase purity of the bulk product was independently confirmed by powder X-ray diffraction (PXRD) and elemental analyses. Elemental analyses (%) calcd for **Mn1**: C, 55.20; H, 3.02; N, 8.39; Found: C, 55.19; H, 3.07; N, 8.41. IR for **Mn1** (KBr, cm^{-1}): 3414.5 (s), 2975.3 (m), 2917.4 (s), 1635.6 (s), 1578.4 (s).1542.3 (s), 1409.8 (s), 1364.7 (s), 842.0 (m), 775.8 (s).

Mn1' was obtained by soaking desolvated **Mn1** in a solution of I_2 in DMSO / H_2O (v / v = 1:1) at 25 °C for 24 h, then washed with ethanol and dried in air. The color of the crystals transforms from yellow to brown (Figure S10), in which, the the valence of Mn changes from II to III was confirmed by X-ray photoelectron spectroscopy (XPS, Figure 2), and the chemical stability was confirmed by PXRD (Figure 3a).

Method for metal ion sensor of **Mn1**: **Mn1** (10.00 mg, 0.02 mmol) was underwent ethanol activation, followed by vacuum drying oven at 40 °C for de-solvation, finally immersing it into 10 mL DMF containing 0.02 mmol metallic nitrate/perchlorate (M = Ag^+, Hg^{2+}, and Zn^{2+}) at room temperature for 24 hours for luminescence measurement.

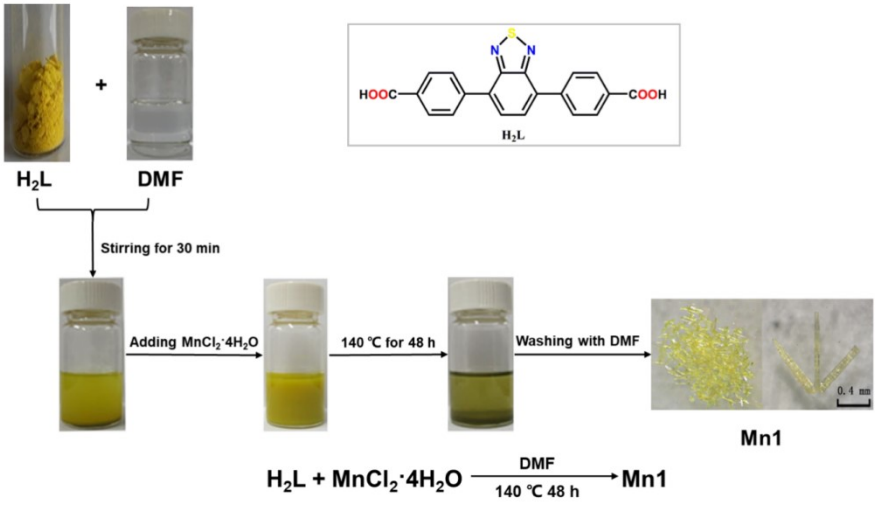

Figure S1. Hydrothermal Synthesis of **Mn1**

Methods

Elemental analyses for C, H, and N were performed on a Vario Micro Cube.

Thermogravimetric analyses (TGA) were performed in a flow of nitrogen at a heating rate of 5 °C min^{-1} using a NETZSCH TG 209 F3.

Infrared spectra were recorded by transmission through KBr pellets containing *ca*. 0.5% of the compounds using a PE Spectrum FT-IR spectrometer (400-4000 cm^{-1}).

X-ray single crystal diffraction data were collected on a Bruker Smart CCD diffractometer. The sample was measured by Mo-Kα (λ = 0.71073 Å) at 293 K. The structures were solved by direct methods and refined by least-squares. The supplementary crystallographic data can be found in the Supporting Information or can be obtained free of charge from the Cambridge Crystallographic Data Centre via http://www.ccdc.cam.ac.uk/data_request/cif (CCDC-2128410 for **Mn1**.)

Powder X-ray diffraction (PXRD) spectra were recorded on either a D8 Advance (Bruker) diffractometer (Cu Kα, λ= 1.54056 Å) at 293 K. The samples were prepared by crushing single crystal and placed on a grooved aluminum plate; patterns were recorded from 3 º to 60 º at a rate of 5 º min^{-1}. Calculated diffraction patterns of the compounds were generated with Mercury software.

X-ray photoelectron spectroscopy (XPS) was performed at the Kratos AXIS Ultra DLD X-ray photoelectron spectrometer. Powder samples were pressed on copper tapes with full coverage. Charge shift was calibrated by setting surface adventitious carbon C1s peak to 284.8 eV.

Gas adsorption isotherms were measured by the Quantachrome Autosorb iQ2 instrument. The samples were outgassed at 110 °C for 4.5 h and then held at 170 °C for 270 min at a pressure of 1×10^{-3} bar. The purpose of the outgas procedure is to drive off acetone and other adsorbed gases, which may impact the isotherm, without materially impacting the **Mn1** samples. At the end of the outgas procedure, the sample was tested for continued outgassing, to ensure completion. Complete outgassing was verified for each sample. All gases used were of 99.999% purity. The N_2 gas sorption isotherm for the desolated solid was monitored at 77 K by using liquid N_2 at each equilibrium pressure by the static volumetric method. Sorption isotherms for CO_2 were measured at both 195 and 273 K by using an acetone/dry ice slush and an ice/water bath, respectively. The sorption properties including the pore volume, pore size, and surface area were analyzed using Autosorb **Mn1** for ASiQwin software.

UV-vis spectra were conducted on an Agilent Cary6000i UV-VIS-NIR spectrophotometer between 200~800 nm. A KBr baseline and a zero-background correction were collected prior to the sample measurements.

Fluorescence spectra were recorded onto the adjustable entrance slits of a FLS980 fluorescence spectrometer (Edinburgh Instrument) equipped with a 450-W continuous wavelength Xe lamp. The signal was detected using Hamamatsu R928P photomultipliers for the 200 ~ 800 nm wavelength region. All excitation and emission spectra were corrected for the spectrometer response.

Electrical conductivity meter was tested by using the ST2643 ultra-high resistance microcurrent tester with a resolution of 0.01×10^{-2} ~ 0.01×10^{-15} Ω. The principle of annular three-electrode method is used to measure solid sheet materials.

RESULTS AND DISCUSSION

Table S1. Crystal structure and properties of MOFs using H_2BTDB

Molecular Formula	Crystal system Space group	Structure description	Framework Structure	Reference
[Mn(BTDB)] $(DMF)_{0.8}$	Orthorhombic *Pccn*	Porosity: 25.6% BET: 184.66 m^2/g, average pore size: 1.79 nm	Columnar chain-like structure	This Work
$[Eu_2(BTDB)_3(H_2O)_4]\cdot 3DMF$	Triclinic *P-1*	Porosity: Not detailed BET: 31.2 m^2/g, average pore size: 2.25 nm	One-dimensional double chain structure expanding into a three-dimensional porous structure	Chem. Eng. J. 2022, 441, 136049
$[Zr_6O_4(OH)_4(BTDB)_6]\cdot 8H_2O\cdot 6DMF$	Cubic *Fmm*	Porosity: Not detailed BET: 430 m^2/g, average pore size: Not detailed	UiO-68 framework structure with large pore apertures	CrystEngComm, 2016,18, 3104-3113
$[Mn_4(BTDB)_2(HCOO)_4(DEF)_2]$	Monoclinic *P2_1/c*	Porosity: Not detailed BET: , Not detailed average pore size: Not detailed	Three-dimensional structure with manganese formate chains	ChemPlusChem. 2017, 82, 1153-1163
[Pb(BTDB)(DMF)]	Monoclinic *P2_1/n*	Porosity: Not detailed BET: , Not detailed average pore size: Not detailed	Two-dimensional layer structure with Pb-O-Pb chains	ChemPlusChem. 2017, 82, 1153-1163
$[Cd_2(BTDB)_2(4,4\text{-bpy})]\cdot DMF$	Triclinic *P-1*	Porosity: 14.1% BET: Not detailed average pore size: Not detailed	Two-fold interpenetrated framework with a pcu topological network	Dalton Trans., 2022, 51, 5983-5988
$[Eu_3(BTDB)_3(\mu_3\text{-}OH)_3(H_2O)]\cdot$solvents	Triclinic *P-1*	Porosity: 19.3% BET: Not detailed average pore size:	3D chain structure	Dalton Trans., 2023, 52, 10567-10573
$[Zn_2(trz)_2(btdb)]\cdot 4DMF$	Tetragonal I4/m	Porosity: 42.7% , BET:586 m^2/g average pore size: 4.0–8.8 Å	Pillared-layer framework with a (4,4)-grid net	Inorg. Chem. Commun., 2021, 129, 108664
Zr-BTDB-fcu-MOF	Cubic *Fmm*	Porosity: Not detailed BET: 2380 m^2/g, average pore size: Not detailed	UiO-68 framework structure	J. Am. Chem. Soc, 2019, 141,18, 7245–7249

Crystal Structures

Table S2. Crystal and structure refinement data for **Mn1**.

Compound	**Mn1**
Formula	$C_{20}H_{10}MnN_2O_4S$
Formula weight	429.30
Crystal system	orthorhombic
Space group	*Pccn*
T (K)	273
a (Å)	35.110(2)
b (Å)	15.8941(5)
c (Å)	7.5210(5)
α (deg)	90
β (deg)	90
γ (deg)	90
V (Å^3)	4197.1(4)
D_c (g cm^{-3})	1.359
F (000)	2064
Z	8
μ (mm^{-1})	0.754
Reflns collected	28733
Unique reflns	3673
R_{int}	0.0904
GOF	1.104
R_1[a] [$I > 2\sigma(I)$]	0.0863
wR_2[b] (all data)	0.2298

Table S3. Selected bond lengths for **Mn1**.

Atom	Atom	Length/Å	Atom	Atom	Length/Å
Mn1	O1	2.200(4)	C00K	C11	1.504(8)
Mn1	O1	2.155(4)	C00K	C15	1.393(9)
Mn1	O2	2.184(4)	C00K	C19	1.366(9)
Mn1	O3	2.122(5)	C1	C2	1.521(7)
Mn1	O4	2.096(5)	C2	C3	1.396(8)
S1	N1	1.604(5)	C2	C7	1.380(8)
S1	N2	1.603(6)	C3	C4	1.383(8)
O1	Mn1	2.155(4)	C4	C5	1.404(9)
O1	Mn1	2.200(4)	C5	C6	1.370(8)
O1	C1	1.290(8)	C6	C7	1.394(8)
O2	Mn1	2.184(4)	C9	C10	1.438(8)
O2	C1	1.221(8)	C10	C11	1.438(9)
O3	Mn1	2.122(5)	C11	C12	1.355(9)
O3	C20	1.240(8)	C12	C13	1.415(8)
O4	C20	1.254(8)	C15	C16	1.401(8)
N1	C9	1.354(8)	C16	C17	1.389(9)
N2	C10	1.331(8)	C17	C18	1.374(9)
C00F	C5	1.484(7)	C17	C20	1.510(8)
C00F	C9	1.425(8)	C18	C19	1.360(9)
C00F	C13	1.360(9)			

Table S4. Selected bond angles for **Mn1**.

Atom	Atom	Atom	Angle/°	Atom	Atom	Atom	Angle/°
O1	Mn1	O1[2]	156.9(2)	C7	C2	C3	120.3(5)
O1	Mn1	O2[3]	83.48(18)	C4	C3	C2	119.5(6)
O2	Mn1	O1[2]	92.58(17)	C3	C4	C5	120.9(5)
O3	Mn1	O1[1]	88.94(18)	C4	C5	C00F	121.7(5)
O3	Mn1	O1[2]	86.19(18)	C6	C5	C00F	120.0(5)
O3	Mn1	O2[3]	157.7(2)	C6	C5	C4	118.1(5)
O4	Mn1	O1[2]	96.21(19)	C5	C6	C7	122.1(6)
O4	Mn1	O1[1]	106.81(19)	C2	C7	C6	119.0(5)
O4	Mn1	O2[3]	96.01(19)	N1	C9	C00F	126.6(5)
O4	Mn1	O3[4]	106.3(2)	N1	C9	C10	111.2(5)
N2	S1	N1	101.3(3)	C00F	C9	C10	122.1(6)
Mn1	O1	Mn1[5]	120.93(18)	N2	C10	C9	114.4(6)
C1	O1	Mn1[1]	131.9(4)	N2	C10	C11	126.0(5)
C1	O1	Mn1[5]	102.7(4)	C11	C10	C9	119.6(6)
C1	O2	Mn1[6]	145.7(4)	C10	C11	C00K	122.2(6)
C20	O3	Mn1[7]	143.3(5)	C12	C11	C00K	121.0(6)
C20	O4	Mn1	118.4(4)	C12	C11	C10	116.7(5)
C9	N1	S1	107.0(4)	C11	C12	C13	122.3(6)
C10	N2	S1	106.1(4)	C00F	C13	C12	124.3(6)
C9	C00F	C5	124.1(5)	C00K	C15	C16	119.9(6)
C13	C00F	C5	121.0(6)	C17	C16	C15	120.2(6)
C13	C00F	C9	114.8(5)	C16	C17	C20	120.9(6)
C15	C00K	C11	122.3(6)	C18	C17	C16	118.6(6)
C19	C00K	C11	119.6(6)	C18	C17	C20	120.5(6)
C19	C00K	C15	118.1(6)	C19	C18	C17	120.8(6)
O1	C1	C2	116.7(6)	C18	C19	C00K	122.4(6)
O2	C1	O1	123.3(5)	O3	C20	O4	127.0(6)
O2	C1	C2	119.9(6)	O3	C20	C17	116.4(6)
C3	C2	C1	118.5(5)	O4	C20	C17	116.7(6)
C7	C2	C1	121.0(5)				

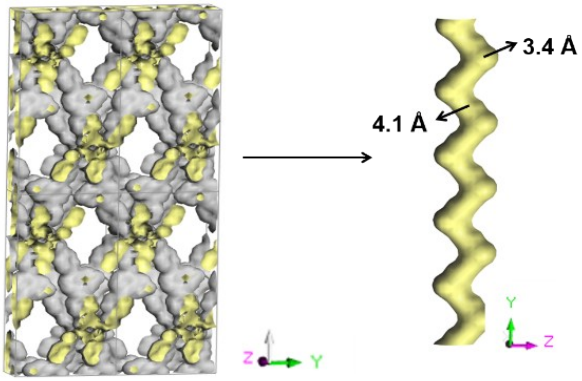

Figure S2 The left- and right-handed alternate two Mn^{II} center short bridging modes forming a stable infinite chain along b axis, and the torsion angle of ligand assembled to the 3D framework along c direction.

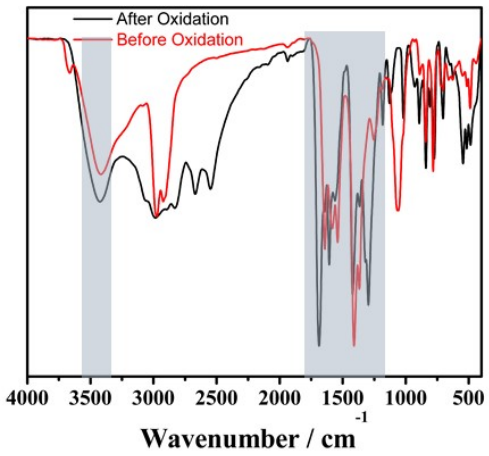

Figure S3. IR spectra of **Mn1** before and after oxidation**.**

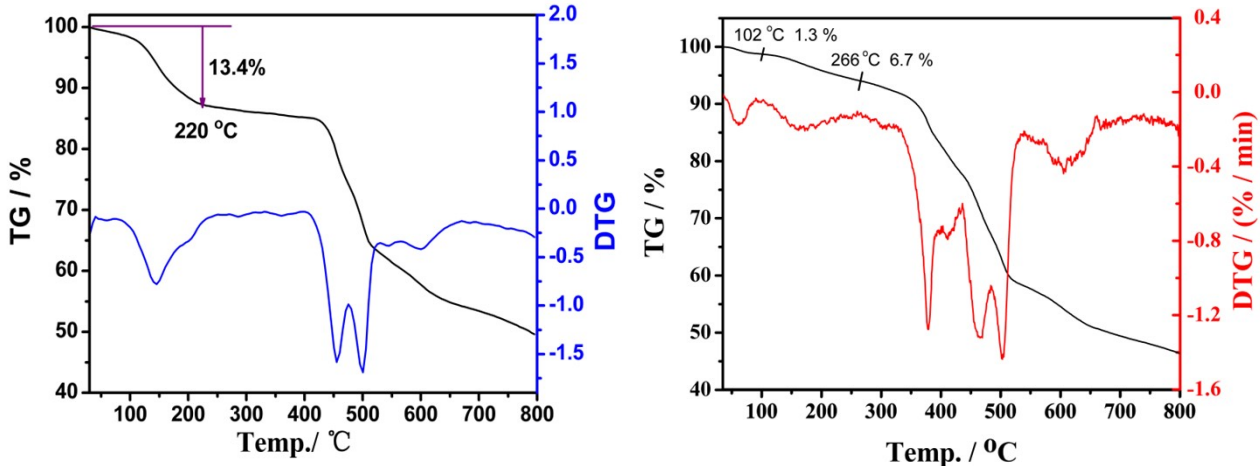

Figure S4. TG curve and DTG of **Mn1** and **Mn1'**.

The thermogravimetric curve shows a time-dependent platform indicating that the guest DMF has been completely removed. Under nitrogen atmosphere, the compound showed significant weight loss with the increase of temperature between 35° and 350°. When the temperature was 102 ℃, there was a weight loss, the weight loss rate was 1.3% (the theoretical value was 1.1%), corresponding to 0.3·H_2O molecules, and there was also a weight loss at 266 ℃. The weight loss rate is 6.7% (theoretical value is 6.4%), corresponding to 0.4·DMSO, and then the mass balance can be maintained up to nearly 350 °C. At higher temperatures, the frame rapidly decomposes and is accompanied by severe weight loss. Finally, at 800 °C, the remaining value is 53.62% of the black residue, which may be manganese oxide.

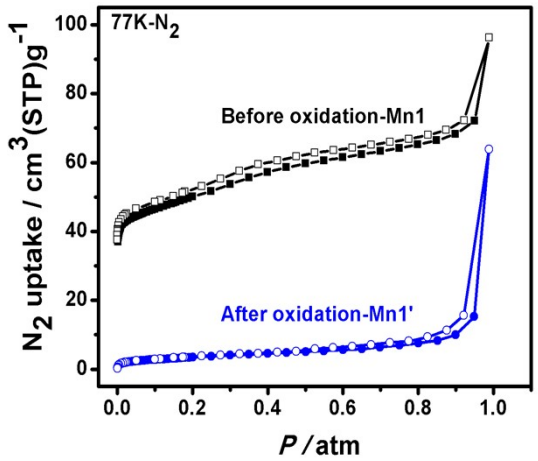

Figure S5. N_2 adsorption / desorption isotherms of **Mn1** before and after oxidation

Titration of iodine content of Mn1 after oxidative modification of Mn^{2+}

The ground 60.00 mg of oxidized **Mn1'** was weighed in two aliquots and immersed in 10 mL of ultrapure water, respectively. The frame of **Mn1'** was destroyed by adding 30 drops of H_2SO_4. Then the pH of the solution was tested at the same time, and a sample was tested by XRD (**Figure S9**). Through the XRD test in the following figure, it can be determined that the frame of **Mn1'** at pH = 1 has been completely destroyed, which indicates that the negative iodide ions in the pore are completely released in the ultra-pure water solution. The solution of the other sample was diluted to 25 mL and poured into an acid bureter. The mass of $K_2Cr_2O_7$ was accurately weighed to 5.00 mg and mixed into 25 mL solution in a conical flask, and then 1 mL of 0.5% starch indicator was added. The solution prepared above was titrated 3 times in parallel to the solution of the reference substance $K_2Cr_2O_7$. When the solution was titrated to blue color and did not fade for 30 s, it was the end point of titration. At this time, the volume of the solution consumed in the bureter was recorded. The following records were recorded: 15.30, 15.27, and 15.31 mL. Pass through the chemical equation is:

$$Cr_2O_7^{2-} + 6I^- + 14H^+ = 2Cr^{3+} + 3I_2 + 7H_2O$$

The concentration of the standard solution prepared by titration was 6.6 mmol/L, corresponding to 12.62 mg I^-/ 60 mg crystal, or 0.1mol I^-/ 0.1mol **Mn1'.** So Mn^{2+} in the oxidized **Mn1'** is completely oxidized to Mn^{3+}. The molecular formula of the oxidized **Mn1'** is $[Mn^{III}L]\cdot 0.3H_2O\cdot 0.4DMSO\cdot I^-$.(**Figure S3)**

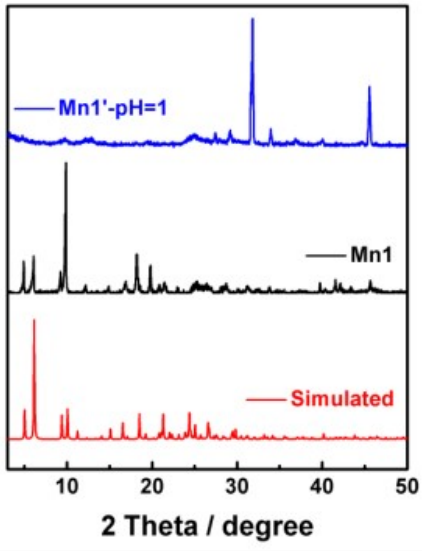

Figure S6. PXRD pattern of **Mn1'** at pH=1

Optical Properties.

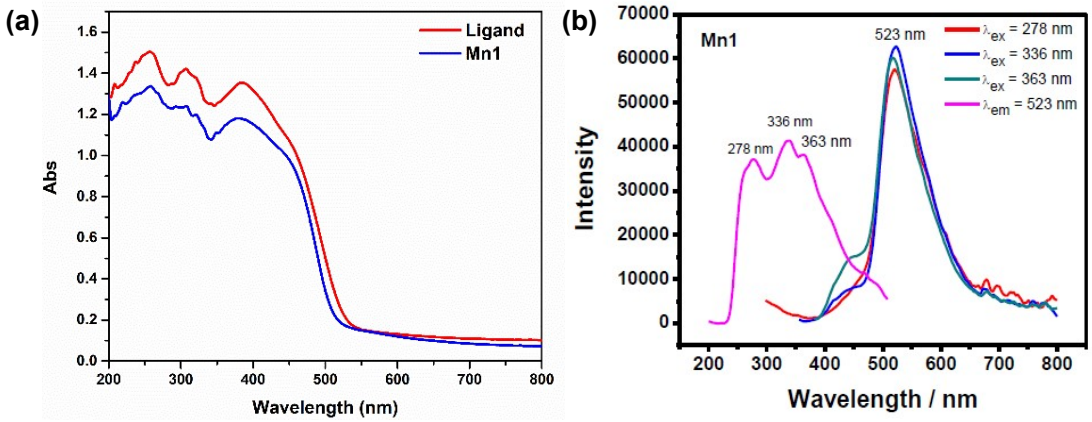

Figure S7. The UV-vis absorption (a) and luminescence (b) spectra of **Mn1** in solid state at room temperature.

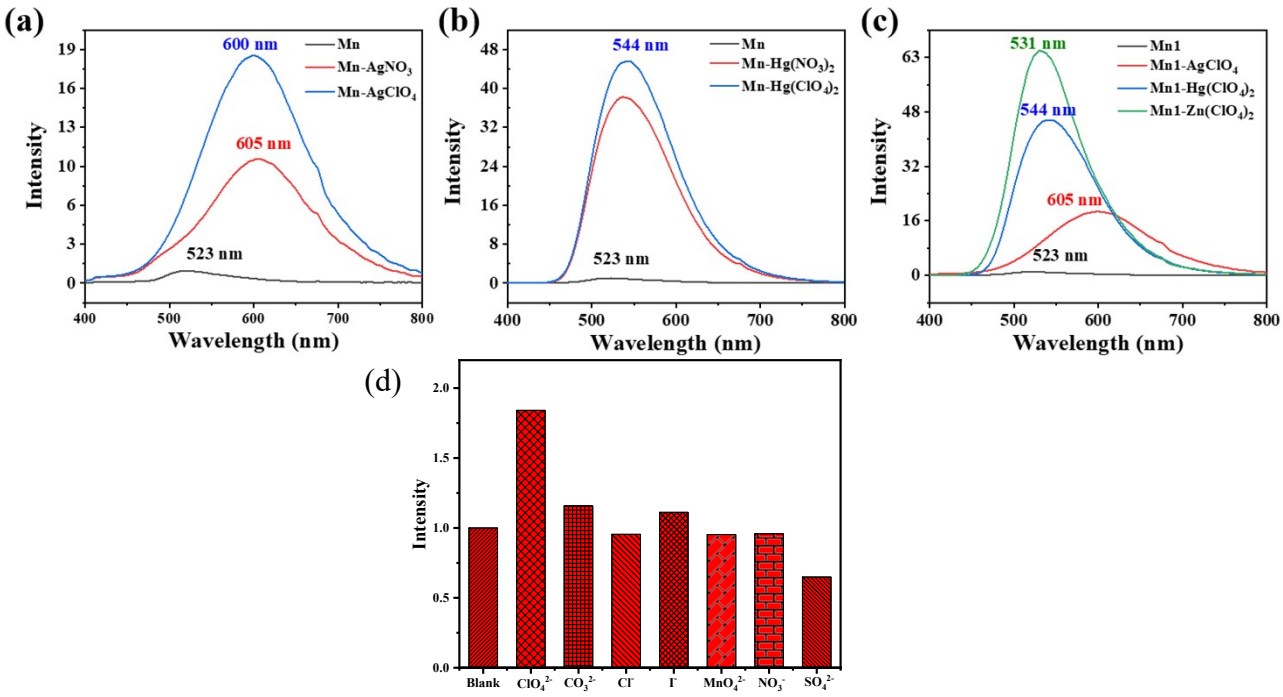

Figure S8. Fluorescence intensity triggered by Ag^{+} (a), Hg^{2+} (b), Zn^{2+} (c), and different anions (d) for turn-on luminescence of **Mn1**

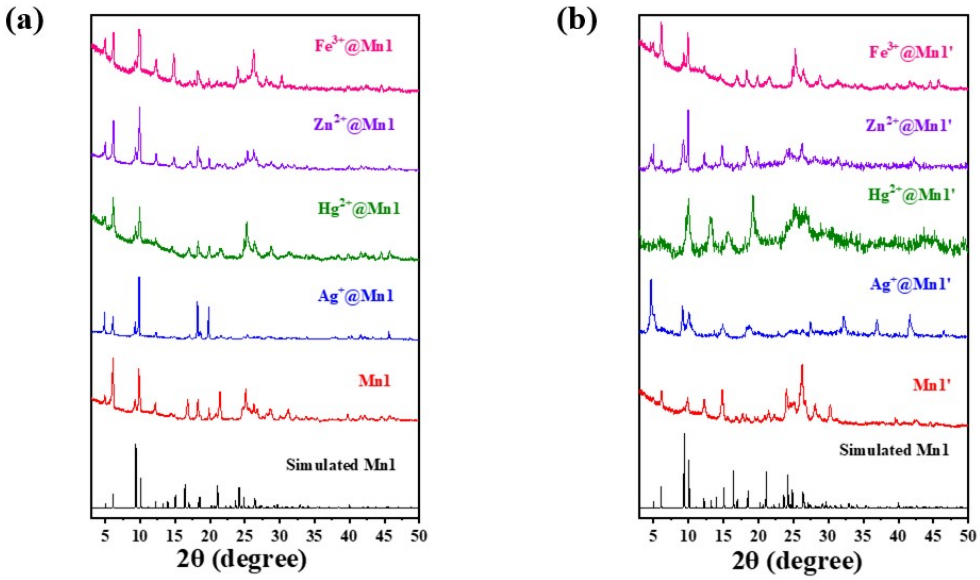

Figure S9. The PXRD patterns of **Mn1** (a) and **Mn1'** (b) treated with different metal salts in solid state at room temperature.

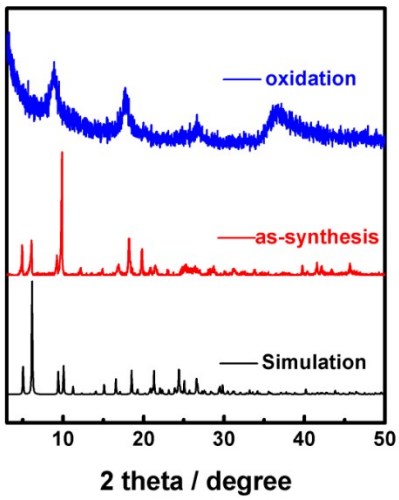

Figure S10 The PXRD patterns of Mn1 before and after oxidation by H_2O_2

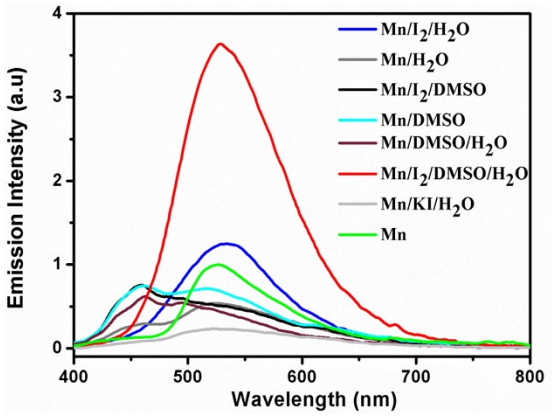

(a)

Samples	Relative intensity
Mn	1
$Mn/I_2/DMSO/H_2O$	3.64
$Mn/I_2/H_2O$	1.25
Mn/DMSO	0.62
$Mn/I_2/DMSO$	0.60
$Mn/DMSO/H_2O$	0.55
Mn/H_2O	0.54
$Mn/KI/H_2O$	0.23

(b)

Figure S11. The fluorescence spectra (a) and a list of the relative emission intensity (b) of **Mn1** treated with different oxidizing agents under λ_{ex} = 336 nm in solid state at room temperature.

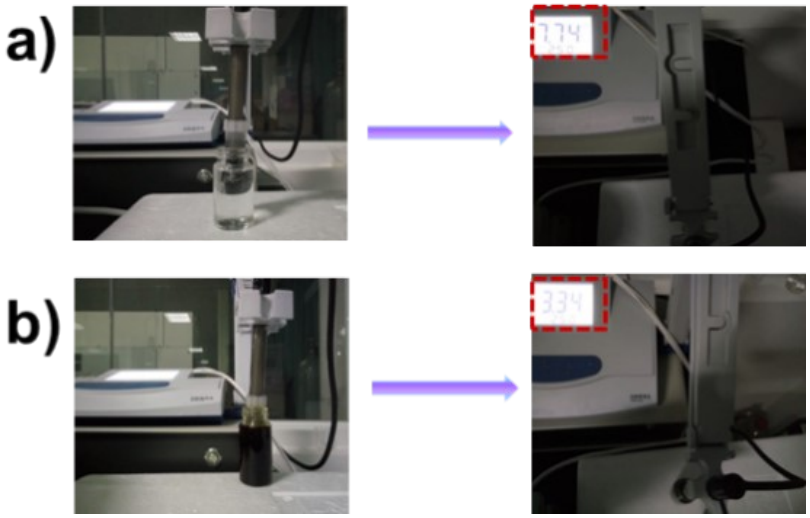

Figure S12. PH tests of the mixed solution in DMSO/H_2O (v/v = 1:1) before (a) and after (b) I_2 immersion.

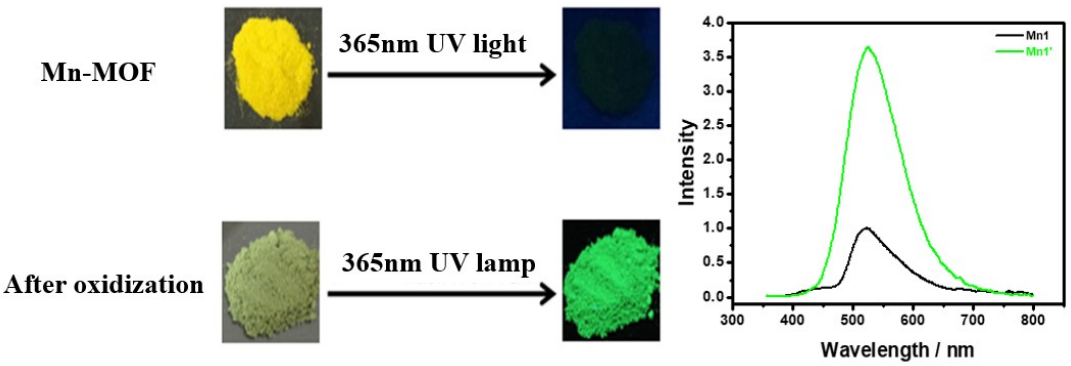

Figure S13. The emission spectra (λ_{ex} = 336 nm) of **Mn1** crystals before and after immersed in the same amount of different metal salt solutions for 5 min at room temperature.

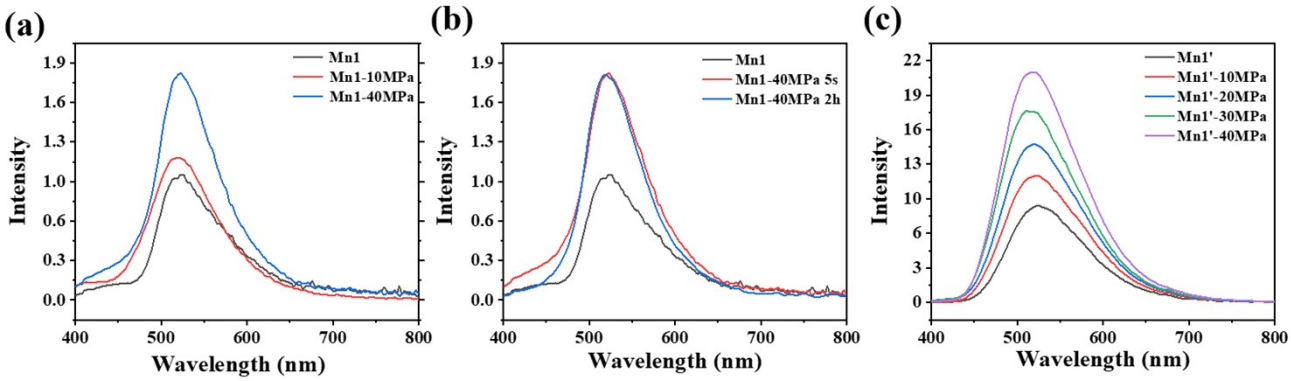

Figure S14. Fluorescence intensity of **Mn1**(a, b) and **Mn1'** (c) under different pressure.

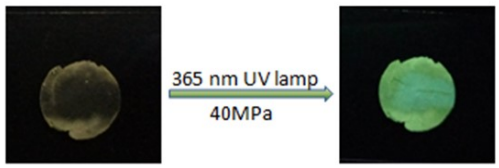

Figure S15. The fluorescence spectra of **Mn1'** under 40 MPa for 5 seconds at room temperature.

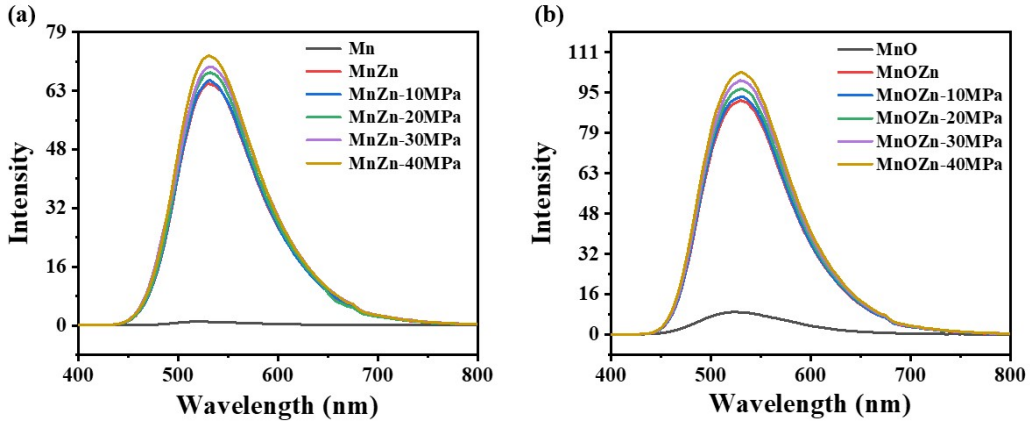

Figure S16. The fluorescence spectra of coupling sensing among $Zn(ClO_4)_2$ under different pressure in **Mn1** and **Mn1'** at λ_{ex} = 336 nm in solid state at room temperature.

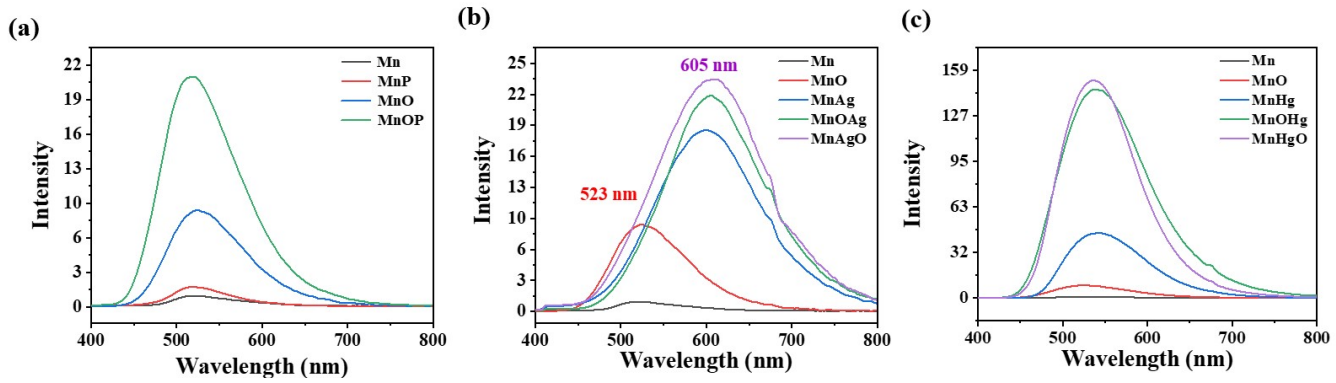

Figure S17. The fluorescence spectra of coupling sensing among $Ag(ClO_4)_2$ and $Hg(ClO_4)_2$ under different pressure in **Mn1** and **Mn1'** at λ_{ex} = 336 nm in solid state at room temperature.

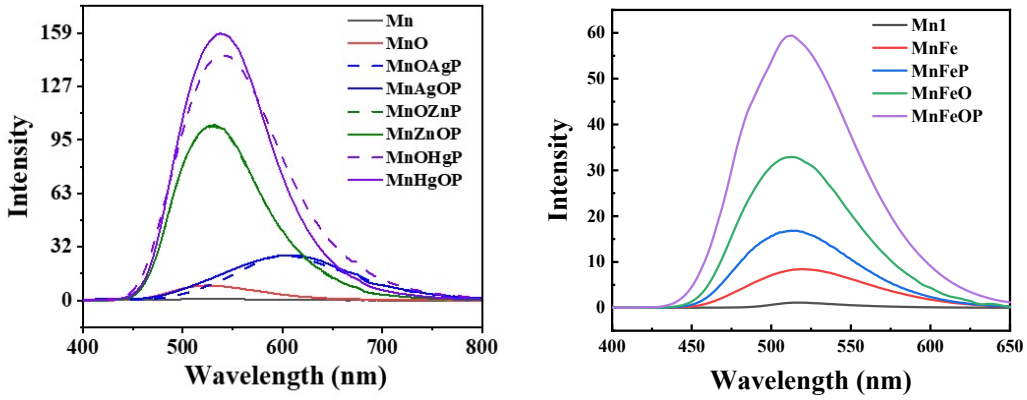

Figure S18. Three kinds of coupling effect on luminescence (λ_{ex} = 336 nm) with $Ag^{+}/Zn^{2+}/Hg^{2+}/Fe^{3+}$/oxidation/pressure.

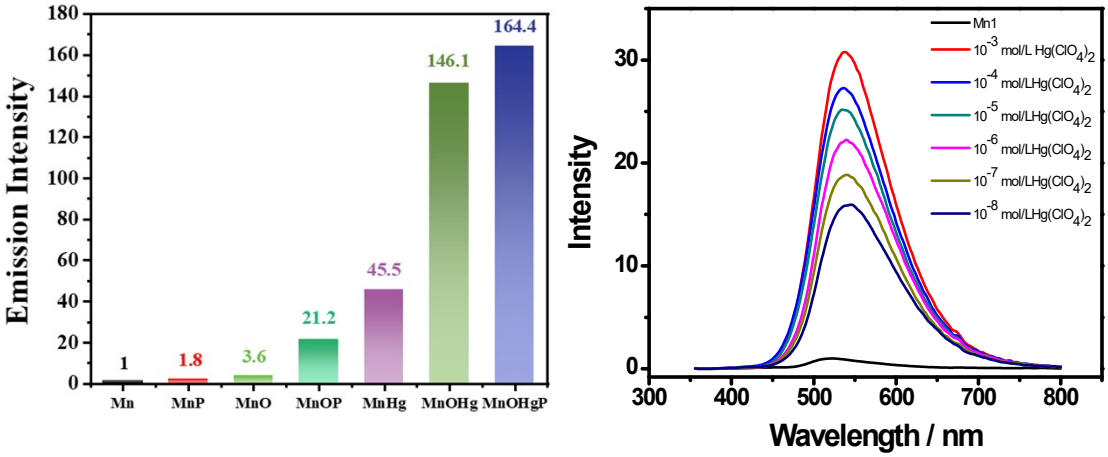

Figure S19: Determination of detection rate and detection limit of $Hg(ClO_4)_2$.

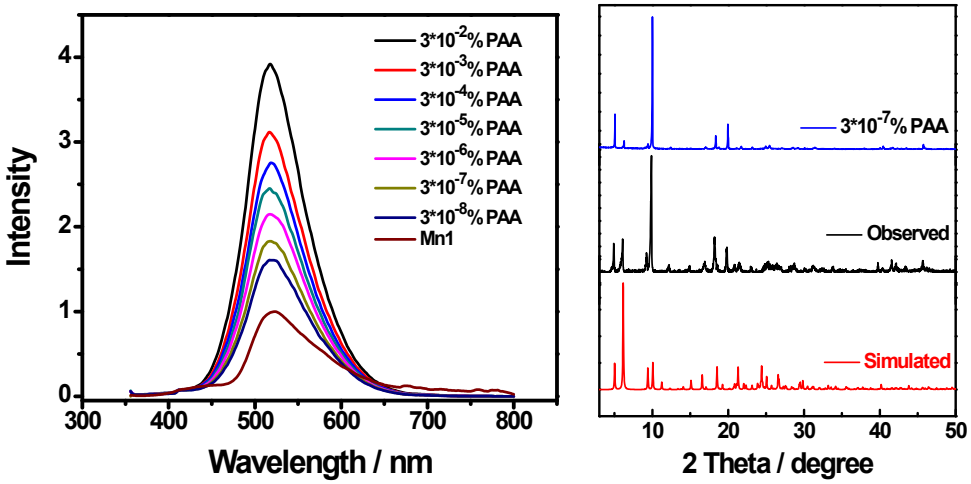

Figure S20: Determination of detection rate and detection limit of the oxidant PAA.

Cycle test: 5mg **Mn1** was put into 10ml of 10mM Ag^{+}, Hg^{2+}, Fe^{3+} solution for 3 hours, and then the fluorescence intensity was tested by taking it out, and then the modified **Mn1** was desorbed of metal ions and the fluorescence intensity was tested, and the fluorescence intensity was tested to third cycles.

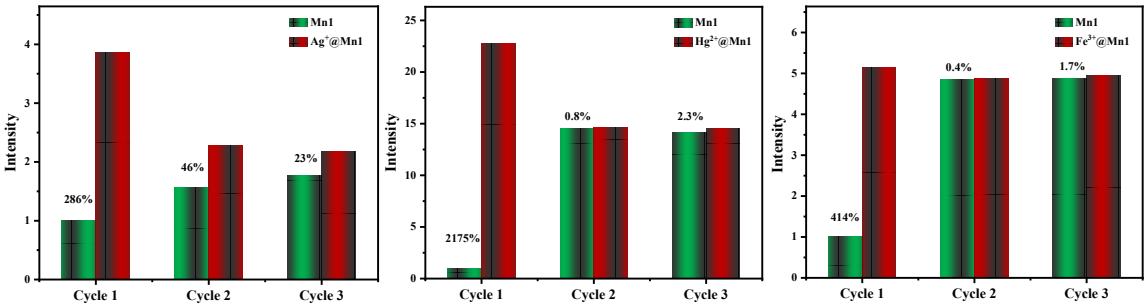

Figure S21 Magnifying efficiency up to third cycle for Ag^{+}, Hg^{2+} and Fe^{3+} detection by **Mn1**.

Computational Methods

H_2BTDB(H_2L) was subjected to structural optimization using Density Functional Theory (DFT), Becke's three-parameter hybrid exchange function, and Lee-Yang-Parr gradient-corrected correlation functional (B3-LYP functional), with a 6-31g** basis set. Excited state calculations were performed using the time-dependent density functional theory (TD-DFT). Both the ground state and excited states incorporated gb3bj dispersion. The solvent effects of water (ε = 78.36) were also taken into consideration using the conductor-like polarizable continuum model (CPCM). Ag^{+}, Zn^{2+}, and Fe^{3+}@H_2L were subjected to structural optimization using Density Functional Theory (DFT) and the PBE0 functional. The C, H, O, N, and S atoms utilized a 6-31g** basis set, while Ag, Zn, and Fe were optimized with the SDD pseudopotential basis set. Excited state calculations were performed using TD-DFT. Both the ground state and excited states incorporated gb3bj dispersion. Tables S5-S12 shows the Cartesian cartesian coordinates of the ground and excited states of each element after DFT calculation.

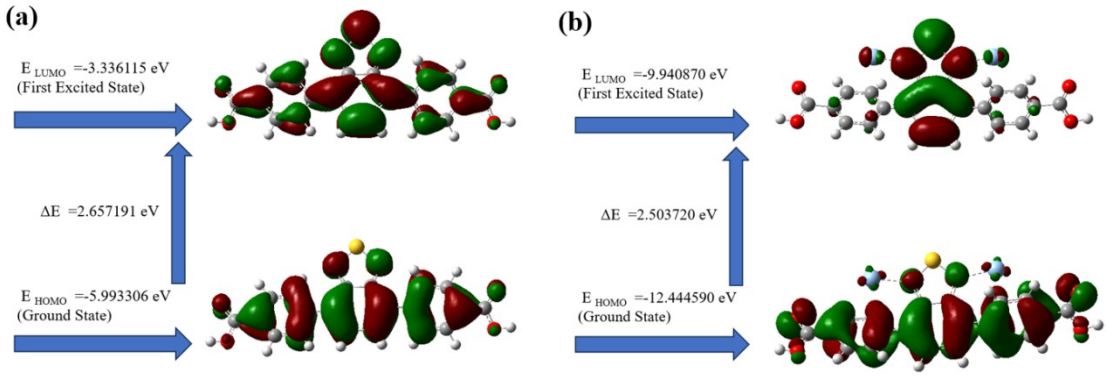

Figure S22. (a): HOMO-LUMO orbit diagram of H_2BTDB(H_2L). (b)HOMO-LUMO orbit diagram of Ag^+@H_2L

Table S5. Coordinates of atoms in the ground state of H_2L

atom	cartesian coordinates (x y z)		
C	-4.99515200	-1.42979800	0.73231700
C	-5.74568500	-0.51643500	-0.01364200
C	-5.08984800	0.47999600	-0.74168200
C	-3.70667700	0.56502700	-0.72950300
C	-2.94136800	-0.35448900	0.00500900
C	-3.61088700	-1.34657400	0.73859600
C	-1.46644700	-0.31321700	-0.00304500
C	-0.70926500	-1.46392700	-0.00161900
C	0.70926500	-1.46392700	0.00161500
C	1.46644700	-0.31321700	0.00304800
C	0.72745900	0.91594600	0.00606500
C	-0.72746000	0.91594700	-0.00605300
C	2.94136800	-0.35448900	-0.00500900
C	3.61088600	-1.34657000	-0.73860400
C	4.99515000	-1.42979400	-0.73232900
C	5.74568500	-0.51643500	0.01363400
C	5.08985000	0.47999100	0.74168100
C	3.70667900	0.56502200	0.72950600
N	-1.25110200	2.14468000	-0.00491500
N	1.25110200	2.14467900	0.00492800
S	0.00000000	3.20107300	0.00002200
C	7.22702500	-0.55779600	0.05866000
O	7.92494900	0.20459800	0.68392400
O	7.74932200	-1.56204500	-0.68832400
C	-7.22702500	-0.55779500	-0.05867200
O	-7.92494800	0.20460300	-0.68393400
O	-7.74932300	-1.56204900	0.68830400
H	-5.49966000	-2.19330900	1.31012000
H	-5.68346800	1.18194800	-1.31459400
H	-3.21174200	1.34442500	-1.29144100
H	-3.03936700	-2.04029700	1.34463000
H	-1.21431600	-2.42289700	-0.02294500
H	1.21431600	-2.42289700	0.02293200
H	3.03936400	-2.04028900	-1.34464100
H	5.49965700	-2.19330100	-1.31013800
H	5.68347100	1.18193900	1.31459600
H	3.21174500	1.34441700	1.29145100
H	8.71150700	-1.50403800	-0.59478700
H	-8.71150900	-1.50404200	0.59476500

Table S6. Coordinates of atoms in the excited state of H_2L

atom	cartesian coordinates (x y z)		
C	4.94283800	-1.63890200	-0.39363200
C	5.73247600	-0.54803700	0.00345200
C	5.10637900	0.64837600	0.38381800
C	3.73265300	0.76340000	0.36705900
C	2.90873200	-0.33194100	-0.01795500
C	3.56815800	-1.53762500	-0.39683600
C	1.46900400	-0.25341600	-0.01694200
C	0.68362400	-1.45145600	-0.01886500
C	-0.68362200	-1.45145700	0.01886300
C	-1.46900300	-0.25341800	0.01694100
C	-0.72893600	0.98243300	0.00244500
C	0.72893500	0.98243400	-0.00244500
C	-2.90873100	-0.33194400	0.01795400
C	-3.56815800	-1.53762800	0.39683300
C	-4.94283700	-1.63890400	0.39362800
C	-5.73247500	-0.54803900	-0.00345400
C	-5.10637800	0.64837400	-0.38381800
C	-3.73265200	0.76339900	-0.36705800
N	1.26123600	2.20627000	-0.01422100
N	-1.26123900	2.20626900	0.01422000
S	-0.00000200	3.30581300	0.00000000
C	-7.21218600	-0.61267500	-0.03347100
O	-7.93286300	0.30737700	-0.35946800
O	-7.69358600	-1.81490100	0.34237400
C	7.21218700	-0.61267300	0.03346800
O	7.93286300	0.30737500	0.35947500
O	7.69358600	-1.81490300	-0.34236800
H	5.41722500	-2.55978800	-0.70306900
H	5.72160300	1.48255000	0.69493900
H	3.26578600	1.69000100	0.65822800
H	2.99359500	-2.38746500	-0.73474100
H	1.18558700	-2.40705200	-0.00816700
H	-1.18558400	-2.40705300	0.00816300
H	-2.99359500	-2.38746800	0.73473700
H	-5.41722500	-2.55979000	0.70306400
H	-5.72160200	1.48255000	-0.69493800
H	-3.26578400	1.69000000	-0.65822600
H	-8.66057200	-1.76932500	0.29442200
H	8.66057100	-1.76932900	-0.29440900

Table S7. Coordinates of atoms in the ground state of $Ag^{+}@H_2L$

atom	cartesian coordinates (x y z)		
C	-5.05560600	1.77837300	-1.03082100
C	-5.74143700	1.08926700	-0.03531200
C	-5.03874200	0.54845700	1.05400500
C	-3.64067600	0.66580700	1.11212200
C	-2.93653700	1.29376200	0.04972400
C	-3.66034500	1.86545400	-0.99634100
C	-1.45815600	1.30011600	0.04345800
C	-0.71172200	2.45350500	0.01504700
C	0.71173900	2.45371500	-0.01540900
C	1.45846500	1.30051700	-0.04356700
C	0.72145300	0.07498700	-0.02401900
C	-0.72088300	0.07473300	0.02412200
C	2.93683800	1.29428300	-0.04993500
C	3.66063300	1.86591000	0.99617400
C	5.05586100	1.77860000	1.03079000
C	5.74165600	1.08926000	0.03540500
C	5.03898100	0.54857000	-1.05396400
C	3.64095700	0.66619900	-1.11225400
N	-1.22786800	-1.16900700	0.02435300
N	1.22887600	-1.16856100	-0.02400700
S	0.00070000	-2.23962200	0.00031600
C	7.22416100	0.88522700	0.05099000
O	7.77994500	0.15229800	-0.73014600
O	7.81871900	1.58267100	1.01553600
C	-7.22400400	0.88562900	-0.05063600
O	-7.77986500	0.15302200	0.73074100
O	-7.81851100	1.58310200	-1.01519300
H	-5.60957800	2.22754500	-1.84882100
H	-5.60444400	0.10811300	1.87192600
H	-3.10981700	0.38948600	2.02328700
H	-3.13202400	2.36086300	-1.80600600
H	-1.22537500	3.41054800	0.02963200
H	1.22508100	3.41091900	-0.03019400
H	3.13230000	2.36139600	1.80578600
H	5.60986700	2.22770600	1.84880300
H	5.60464200	0.10801100	-1.87179300
H	3.11013800	0.38988600	-2.02344000
H	8.77655100	1.40629500	0.96821400
H	-8.77639100	1.40703900	-0.96768500
Ag	3.55159200	-1.47715500	-0.14702800
Ag	-3.55238600	-1.47718200	0.14676900

Table S8. Coordinates of atoms in the excited state of $Ag^{+}@H_2L$

atom	cartesian coordinates (x y z)		
C	-5.01003500	2.13653700	-0.64524100
C	-5.68901400	1.22198800	0.16197700
C	-4.97201100	0.37616200	1.03331400
C	-3.58137600	0.41094400	1.04635100
C	-2.87626400	1.29082800	0.16934300
C	-3.62086600	2.18026800	-0.63267400
C	-1.42735500	1.25435100	0.07245600
C	-0.69214700	2.45344600	0.00749000
C	0.69215100	2.45344500	-0.00746800
C	1.42735700	1.25434900	-0.07244300
C	0.70219900	0.01821700	-0.04274300
C	-0.70219800	0.01821800	0.04274800
C	2.87626600	1.29082600	-0.16933500
C	3.62087300	2.18026600	0.63268000
C	5.01004200	2.13653900	0.64523600
C	5.68901700	1.22199400	-0.16199000
C	4.97201000	0.37616600	-1.03332100
C	3.58137500	0.41094400	-1.04634700
N	-1.25176400	-1.23078100	0.05010200
N	1.25176200	-1.23078300	-0.05010700
S	-0.00000200	-2.34129100	-0.00000600
C	7.17529800	1.07065800	-0.14567000
O	7.71591100	0.10690900	-0.63524900
O	7.78455800	2.07486500	0.47145200
C	-7.17529500	1.07064600	0.14564400
O	-7.71591000	0.10691100	0.63524800
O	-7.78455500	2.07486300	-0.47146300
H	-5.57347000	2.80210400	-1.29125600
H	-5.53072100	-0.24847500	1.72601200
H	-3.03000000	-0.11785800	1.82208100
H	-3.10117700	2.86529600	-1.29591900
H	-1.22370200	3.39935300	0.03408300
H	1.22370800	3.39935100	-0.03405500
H	3.10118700	2.86529100	1.29592900
H	5.57348000	2.80210600	1.29124800
H	5.53071600	-0.24847100	-1.72602400
H	3.02999400	-0.11786200	-1.82207300
H	8.74571100	1.90788100	0.45901700
H	-8.74570800	1.90788700	-0.45901300
Ag	3.41570400	-1.59994200	0.28586600
Ag	-3.41570700	-1.59993300	-0.28586300

Table S9. Coordinates of atoms in the ground state of $Zn^{2+}@H_2L$

atom	cartesian coordinates (x y z)		
S	-0.00341500	2.37951500	1.22999700
N	1.24629300	1.38314200	0.80462700
N	-1.27149000	1.40978400	0.79770100
C	1.45623800	-0.91277200	-0.07573800
C	-2.96679800	-0.97685800	-0.03271300
C	5.69962900	-1.25636700	-0.02503600
C	5.06400300	-0.40524700	0.89826900
H	5.65851700	0.13203500	1.62781100
C	3.69012900	-0.26048500	0.86885600
H	3.20690200	0.38967300	1.58447700
C	2.90222500	-0.99707100	-0.06575400
C	3.56643900	-1.86748700	-0.97876400
H	2.99956700	-2.40338800	-1.73102600
C	4.93867500	-1.98965200	-0.96178600
H	5.45737100	-2.63543900	-1.66160200
C	0.71398700	0.24739500	0.37365600
C	-0.76225700	0.26634400	0.35684100
C	-1.52019600	-0.89659600	-0.06401200
C	-0.73450600	-1.98135800	-0.49974700
H	-1.23237900	-2.87171600	-0.86319300
C	0.66020200	-1.98257400	-0.52390800
H	1.14843700	-2.88830400	-0.86307200
C	-3.79360400	0.18738200	-0.06781100
H	-3.33876000	1.16546400	-0.12587900
C	-5.17024600	0.07784200	-0.05868500
H	-5.79375300	0.96277700	-0.10545300
C	-5.77263600	-1.19362300	-0.00877900
C	-4.97496300	-2.35738000	0.05442100
H	-5.46571900	-3.32121000	0.13072300
C	-3.60170200	-2.25302000	0.02648100
H	-3.00926800	-3.15613300	0.10757100
C	7.18331700	-1.45447200	-0.03464300
O	7.70555100	-2.35612800	-0.65582900
O	7.83167700	-0.55793500	0.71593300
H	8.78793200	-0.76234600	0.68469800
C	-7.25877300	-1.36979500	0.02436600
O	-7.77080400	-2.42486100	0.33433600
O	-7.92123600	-0.25417000	-0.29694300
H	-8.88067600	-0.43514500	-0.23379500
Zn	0.20054500	4.37335100	-0.84868500

Table S10. Coordinates of atoms in the excited state of $Zn^{2+}@H_2L$

atom	cartesian coordinates (x y z)		
S	0.86402266	0.84985834	0.00000000
N	2.11944566	-0.22921166	-0.24679300
N	-0.46332334	-0.17844066	-0.40385200
C	2.30709766	-2.60030366	-0.91147100
C	-2.08589134	-2.69142166	-0.90688200
C	6.57736666	-2.75168066	-1.05550900
C	5.94852066	-1.83216666	-0.21889100
H	6.55661266	-1.17887166	0.39353400
C	4.56264666	-1.76350666	-0.17683900
H	4.06769366	-1.03255266	0.44631200
C	3.77641666	-2.62326066	-0.96518500
C	4.43241966	-3.53151466	-1.81853100
H	3.85031366	-4.16732266	-2.47526800
C	5.81487766	-3.59322766	-1.86344500
H	6.33201266	-4.27933766	-2.52426500
C	1.56720966	-1.43304966	-0.57801200
C	0.10825766	-1.43517966	-0.63277300
C	-0.61211734	-2.61185566	-0.93210900
C	0.16300366	-3.73356566	-1.24971800
H	-0.34042034	-4.64956866	-1.53189400
C	1.55791066	-3.72846166	-1.23884400
H	2.07870266	-4.65207866	-1.46102100
C	-2.89744434	-1.54846666	-1.02255000
H	-2.42540634	-0.57680566	-1.04095400
C	-4.28201834	-1.65371266	-1.04575600
H	-4.90481834	-0.77274166	-1.13509700
C	-4.88967334	-2.90201666	-0.94522100
C	-4.10505534	-4.04420366	-0.80095600
H	-4.60326234	-5.00189066	-0.70236400
C	-2.72475834	-3.94029066	-0.77274800
H	-2.13511534	-4.83500866	-0.61516300
C	8.04017966	-2.85658566	-1.15138000
O	8.66468966	-3.54833966	-1.94842500
O	8.66778766	-2.05619766	-0.22991800
H	9.64994866	-2.15408666	-0.34327100
C	-6.34890834	-3.07397066	-0.97749300
O	-6.95045834	-4.14162466	-1.01342100
O	-7.00150834	-1.86661966	-0.98267500
H	-7.97982134	-2.03634266	-1.01729000
Zn	0.13691866	0.56238234	-2.36128400

Table S11. Coordinates of atoms in the ground state of $Fe^{3+}@H_2L$

atom	cartesian coordinates (x y z)		
C	-5.06049500	-2.02255400	0.62333800
C	-5.79394800	-1.05551100	-0.09943700
C	-5.11272000	0.02827400	-0.70098100
C	-3.68227600	0.14051600	-0.62640900
C	-2.93187700	-0.93813300	0.03474100
C	-3.65649100	-1.98189200	0.64940400
C	-1.48199000	-0.92618200	0.04952000
C	-0.70197600	-2.09854400	0.04188800
C	0.70216300	-2.09850700	-0.04260900
C	1.48213000	-0.92609500	-0.05000600
C	0.71978400	0.30327400	-0.02273100
C	-0.71972600	0.30327200	0.02246500
C	2.93199100	-0.93791500	-0.03515000
C	3.65673500	-1.98172100	-0.64969100
C	5.06067700	-2.02259900	-0.62324200
C	5.79408300	-1.05556900	0.09964400
C	5.11282700	0.02836600	0.70087900
C	3.68236200	0.14071400	0.62609300
N	-1.21815900	1.55095300	0.07228300
N	1.21815700	1.55103100	-0.07206700
S	-0.00007200	2.67784900	0.00028700
C	7.30349900	-1.02263100	0.11432400
O	7.64044000	0.07942200	-0.30718800
O	7.95599900	-2.05992900	0.45462800
C	-7.30334400	-1.02252600	-0.11388000
O	-7.64065800	0.07977300	0.30661900
O	-7.95570600	-2.06027900	-0.45324300
H	-5.57788400	-2.84365100	1.12472300
H	-5.68568200	0.75703300	-1.28059800
H	-3.25215500	0.49486400	-1.58219400
H	-3.14446900	-2.78299100	1.18004200
H	-1.19128300	-3.07098900	0.04764600
H	1.19150800	-3.07093200	-0.04848000
H	3.14470000	-2.78267200	-1.18053900
H	5.57808600	-2.84385600	-1.12434500
H	5.68574500	0.75720500	1.28043100
H	3.25235500	0.49487900	1.58205000
H	8.94543200	-1.99539600	0.39385100
H	-8.94513600	-1.99579600	-0.39247800
Fe	3.16145400	1.94028000	-0.30061400
Fe	-3.16180400	1.93997800	0.30054800

Table S12. Coordinates of atoms in the excited state of $Fe^{3+}@H_2L$

atom	cartesian coordinates (x y z)		
C	2.22379602	1.72804530	0.00000000
C	2.96592702	2.70757930	0.69731400
C	2.29449602	3.80802130	1.27398600
C	0.86346002	3.91966130	1.20060900
C	0.09750602	2.83589530	0.56232600
C	0.81914802	1.77568230	-0.02581700
C	-1.35291598	2.84257530	0.56086300
C	-2.12942698	1.66787330	0.58519100
C	-3.53391098	1.66552430	0.67061900
C	-4.31640798	2.83688730	0.66716200
C	-3.55633998	4.06673030	0.63233200
C	-2.11798798	4.06892630	0.58264400
C	-5.76586998	2.82520030	0.65076900
C	-6.49198198	1.78176230	1.26530400
C	-7.89547598	1.73942730	1.23612100
C	-8.62899598	2.70171830	0.50541500
C	-7.94804798	3.78564630	-0.09720100
C	-6.51767498	3.89918530	-0.01919900
N	-1.61931798	5.31541130	0.53229400
N	-4.05699498	5.31290730	0.67703900
S	-2.83777298	6.44023130	0.60827800
C	-10.13846998	2.73007630	0.48517200
O	-10.47135398	3.82812430	0.92123200
O	-10.79088398	1.69922230	0.12868300
C	4.47653302	2.73163330	0.70637500
O	4.83273602	3.83036130	0.29468700
O	5.11578002	1.68354330	1.04369600
H	2.73523802	0.89271930	-0.48386900
H	2.87195502	4.55335230	1.82766200
H	0.42873702	4.33593330	2.13606900
H	0.30201102	0.96040430	-0.52910800
H	-1.63815898	0.69646630	0.58730400
H	-4.02112398	0.69208530	0.68555000
H	-5.97980498	0.98080930	1.79610100
H	-8.41281598	0.91953030	1.73961400
H	-8.52000998	4.51307630	-0.67953600
H	-6.08349898	4.25928630	-0.97223000
H	-11.78069998	1.76262130	0.18760400
H	6.10598402	1.73799130	0.98681700
Fe	-6.00120598	5.69869330	0.89556300
Fe	0.33217302	5.69522930	0.32520500

Conductivity Properties

Impedance test: 400uL ethanol, 80uLH_2O and 20uLNaFion were added into 5mg **Mn1** and I_2@**Mn1**, respectively, and ultrasonic was performed for half an hour each time to make them disperse evenly. It is then loaded on carbon paper 0.5cm×1cm. The voltage is 1.5V and the electrolyte is 1M potassium hydroxide solution. The experimental data were fitted by Zview software.

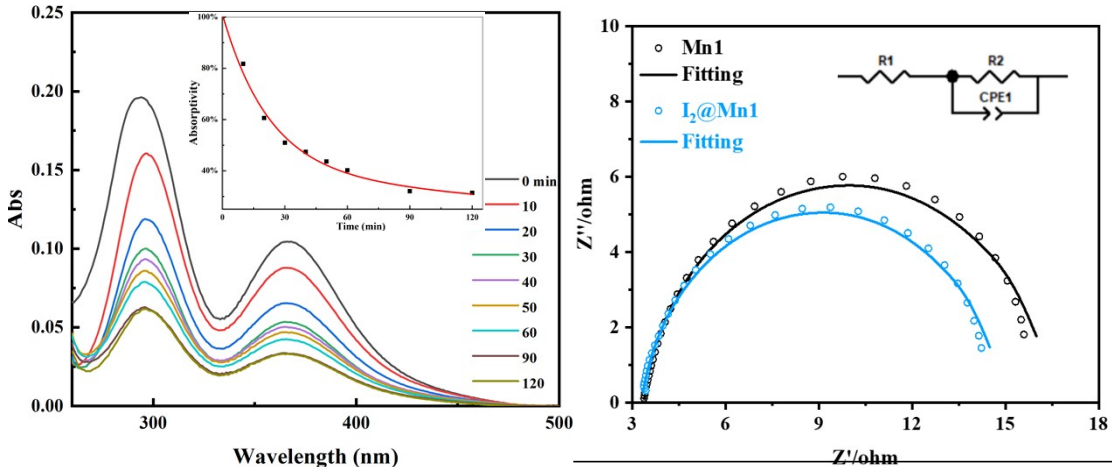

Figure S23 (a) Time-depend iodine uptake and (b) EIS Nyquist plots of **Mn1** before and after adsorption of I_2.

Table S13. Zn@Mn1 conductivity

Height (mm)	Pressure (Mpa)	Specific resistance (TΩ-cm)	specific conductance(pS/cm)
0.67	2	26.12	0.038285714
0.59	4	30.68	0.032596685
0.56	6	30.00	0.033333333
0.54	8	29.81	0.033540373
0.52	10	28.27	0.035374150
0.51	12	28.43	0.035172414
0.50	14	28.20	0.035460993
0.48	16	29.17	0.034285714
0.48	18	28.96	0.034532374
0.47	20	28.94	0.034558824

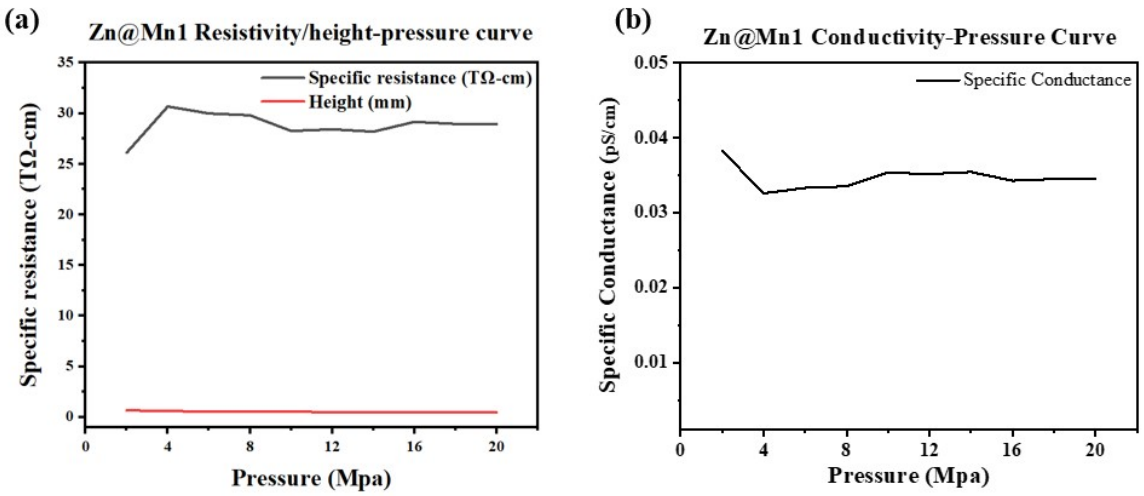

Figure S24: (a)The resistivity/height-pressure curve of **Zn@Mn1**. (b)The conductivity pressure curve of **Zn@Mn1**

Table S14. Mn1' conductivity

Height (mm)	Pressure (Mpa)	Specific resistance (MΩ-cm)	specific conductance(uS/cm)
0.56	2	548.21	0.001824104
0.47	4	453.19	0.002206573
0.44	6	418.18	0.002391304
0.41	8	407.32	0.002455090
0.40	10	387.50	0.002580645
0.39	12	374.36	0.002671233
0.37	14	381.08	0.002624113
0.36	16	375.00	0.002666667
0.35	18	374.29	0.002671756
0.34	20	373.53	0.002677165

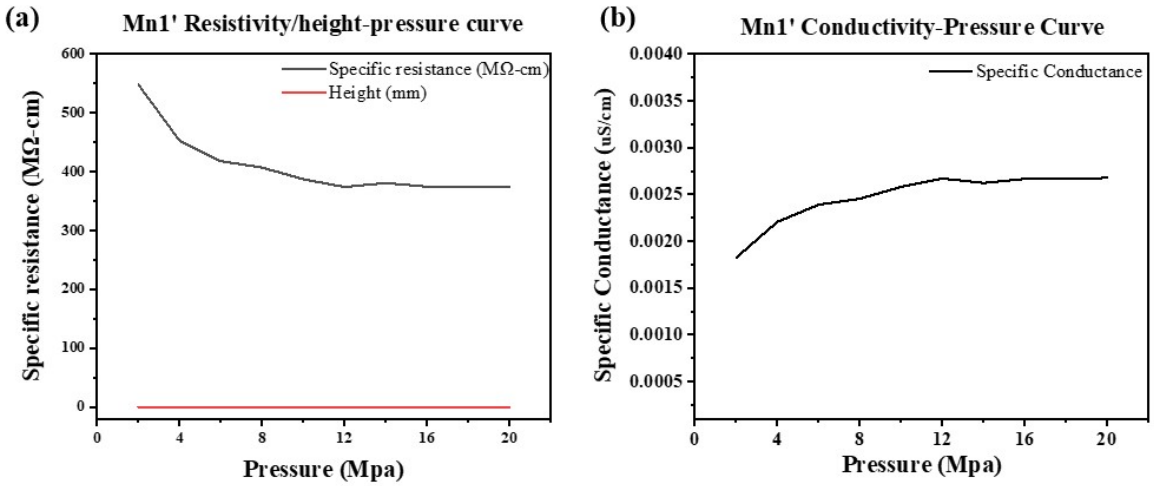

Figure S25: (a)The resistivity/height-pressure curve of **Mn1'**. (b)The conductivity pressure curve of **Mn1'**

Table S15. Zn@Mn1' conductivity

Height (mm)	Pressure (Mpa)	Specific resistance (MΩ-cm)	specific conductance(uS/cm)
1.07	2	12.07	0.082881487
0.91	4	11.95	0.083716651
0.84	6	13.10	0.076363636
0.80	8	14.44	0.069264069
0.76	10	15.57	0.064243449
0.74	12	17.35	0.057632399
0.72	14	18.44	0.054216867
0.70	16	20.31	0.049226442
0.69	18	21.32	0.046906866
0.68	20	22.72	0.044012945

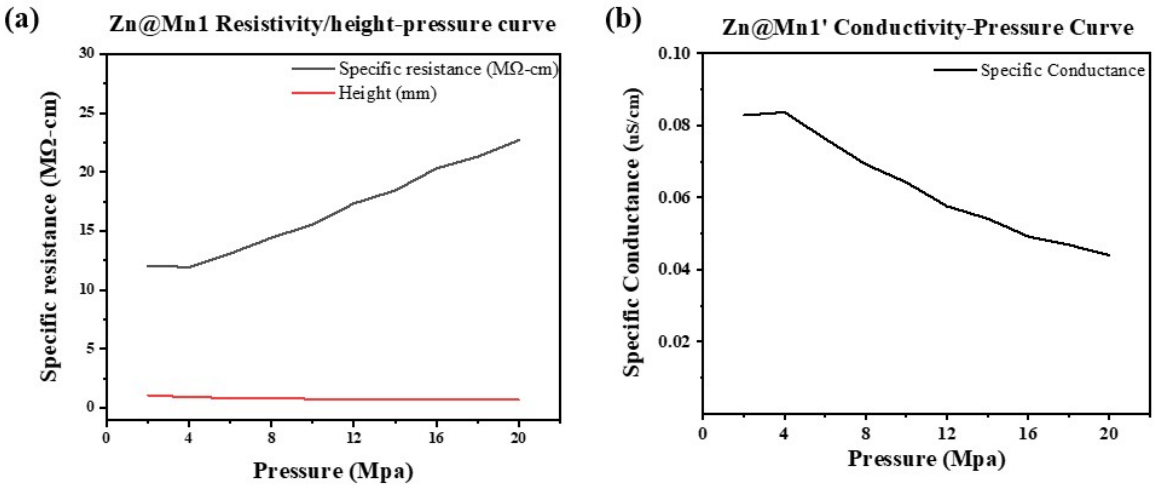

Figure S26: (a)The resistivity/height-pressure curve of **Zn@Mn1'**. (b)The conductivity pressure curve of **Zn@Mn1'**